

Heavy quark bound states above deconfinement

I. M. Narodetskii, Yu. A. Simonov, A. I. Veselov

Institute of Theoretical and Experimental Physics, Moscow 117218, Russia

Abstract

A comprehensive study of the color singlet heavy quark states J/ψ , Υ and Ω_{bbb} above T_c is given. We use the Field Correlator Method (FCM) for nonperturbative $Q\bar{Q}$ potentials and the screened Coulomb potential with the T -dependent Debye mass computed up to two loops in the deconfined phase of QCD. We calculate binding energies and melting temperatures of heavy mesons and baryons in the deconfined phase of quark-gluon plasma and the J/ψ and Υ disintegration cross sections via the gluon absorption.

PACS numbers: 11.25 Sq, 12.38Lg, 12.38.Mh, 14.40.Pq, 25.75.Nq

1 Introduction

Early applications of in-medium heavy-quark potentials have employed a phenomenological ansatz to implement color-screening effects into the one-gluon-exchange (Coulomb) potential [1]. The temperature dependence of this potential is encoded in the Debye mass $m_D(T)$. If Debye screening of the Coulomb potential above the temperature of deconfinement T_c is strong enough, then J/ψ production in A+A collisions will be suppressed. Therefore the gold-plated signature of deconfinement in the Quark-Gluon Plasma (QGP) was thought to be the J/ψ suppression [2]. Indeed, applying the Bargmann condition [3] for the screened Coulomb potential at $T = T_c$

$$V_C(r) = -\frac{4}{3} \cdot \frac{\alpha_s(r)}{r} \cdot e^{-m_D(T_c)r}, \quad (1)$$

we obtain the simple estimate for the number of, say, $c\bar{c}$ S -wave bound states

$$n \leq \mu_c \int_0^\infty |V_C(r)| r dr = \frac{4\alpha_s}{3} \cdot \frac{\mu_c}{m_D(T_c)}, \quad (2)$$

where μ_c is the constituent mass of the c -quark and for the moment we neglect the r -dependence of α_s . Taking $\mu_c = 1.4$ GeV and $\alpha_s = 0.39$, we conclude that if $m_D(T_c) \geq 0.7$ GeV, there is no J/ψ bound state. Parenthetically, we note that for the potential (1) no light or strange mesons ($\mu \sim 300 - 500$ MeV) survive. But this is not the full story.

There is a significant change of views on physical properties and underlying dynamics of quark-gluon plasma (QGP), produced at RHIC, see, *e.g.*, [4] and references therein.

Instead of behaving like a gas of free quasiparticles – quarks and gluons, the matter created in RHIC interacts much more strongly than originally expected. It is more appropriate to describe the nonperturbative (NP) properties of the QCD phase close to T_c in terms of the NP part of the QCD force rather than a strongly coupled Coulomb force.

In the QCD vacuum, the NP quark–antiquark potential is $V = \sigma r$. At $T \geq T_c$, $\sigma = 0$, but that does not mean that the NP potential disappears. In a recent paper [5] we calculated binding energies for the lowest $Q\bar{Q}$ and QQQ eigenstates ($Q = c, b$) above T_c using the NP $Q\bar{Q}$ potential derived in the Field Correlator Method (FCM) [6] and the screened Coulomb potential. The Debye radii were calculated for pure gluodynamics using Eqs. (28),(29) of Ref. [7] and the parameters given there in. In the present paper we refine the results of [5] and, in particular, extend our analysis to the case of the running $\alpha_s(r)$ [8]. We also calculate the dissociation cross sections of J/ψ and Υ in collisions with gluons. Here as in Ref. [5] the Debye mass is evaluated in quenched QCD (the number of light flavors $n_f = 0$, $T_c = 275$ MeV), the similar results using the Debye mass evaluated for two light flavors ($T_c = 165$ MeV) are presented in Ref. [9].

2 Field correlator method as applied to finite temperatures

The NP quark–antiquark potential can be studied through the modification of the correlator functions, which define the quadratic field correlators of the nonperturbative vacuum fields:

$$\langle \text{tr } F_{\mu\nu}(x)\Phi(x,0)F_{\lambda\sigma}(0) \rangle = \mathcal{A}_{\mu\nu;\lambda\sigma} D(x) + \mathcal{B}_{\mu\nu;\lambda\sigma} D_1(x),$$

where $\mathcal{A}_{\mu\nu;\lambda\sigma}$ and $\mathcal{B}_{\mu\nu;\lambda\sigma}$ are the two covariant tensors constructed from $g_{\mu\nu}$ and $x_\mu x_\nu$ [6], $\Phi(x,0)$ is the Schwinger parallel transporter, x is Euclidian. At $T \geq T_c$, one should distinguish the color electric correlators $D^E(x)$, $D_1^E(x)$ and color magnetic correlators $D^H(x)$, $D_1^H(x)$. Above T_c , the color electric correlator $D^E(x)$ that defines the string tension at $T = 0$ becomes zero [10] and, correspondingly, $\sigma^E = 0$. The color magnetic correlators $D^H(x)$ and $D_1^H(x)$ do not produce static quark–antiquark potentials, they only define the spatial string tension $\sigma_s = \sigma^H$ and the Debye mass $m_d \propto \sqrt{\sigma_s}$ that grows with T .

The main source of the NP static $Q\bar{Q}$ potential at $T \geq T_c$ originates from the color–electric correlator function $D_1^E(x)$:

$$V_{\text{np}}(r, T) = \int_0^{1/T} d\nu (1 - \nu T) \int_0^r \lambda d\lambda D_1^E(x). \quad (3)$$

In the confinement region the function $D_1^E(x)$ was calculated in [11]:

$$D_1^E(x) = B \frac{\exp(-M_0 x)}{x}, \quad (4)$$

where $B = 6\alpha_s^f \sigma_f M_0$, α_s^f being the freezing value of the strong coupling constant to be specified later, σ_f is the string tension at $T = 0$, and the parameter M_0 has the meaning

of the gluelump mass. In what follows we take $\sigma_f = 0.18 \text{ GeV}^2$ and $M_0 = 1 \text{ GeV}$. Above T_c the analytical form of D_1^E should stay unchanged at least up to $T \sim 2 T_c$. The only change is $B \rightarrow B(T) = \xi(T)B$, where the T -dependent factor

$$\xi(T) = \left(1 - 0.36 \frac{M_0}{B} \frac{T - T_c}{T_c}\right) \quad (5)$$

is determined by lattice data [12]. Integrating Eq. (3) over λ , one obtains

$$V_{np}(r, T) = \frac{B(T)}{M_0} \int_0^{1/T} (1 - \nu T) \left(e^{-\nu M_0} - e^{-\sqrt{\nu^2 + r^2} M_0}\right) d\nu = V(\infty, T) - V(r, T), \quad (6)$$

where

$$V(\infty, T) = \frac{B(T)}{M_0^2} \left[1 - \frac{T}{M_0} \left(1 - \exp\left(-\frac{M_0}{T}\right)\right)\right], \quad (7)$$

and

$$V(r, T) = \frac{B(T)}{M_0} \int_0^{1/T} (1 - \nu T) \exp(-\sqrt{\nu^2 + r^2} M_0) d\nu. \quad (8)$$

The approximate expression

$$V(r, T) \approx \frac{B(T)}{M_0^2} \left(K_1(x)x - \frac{T}{M_0} \exp(-x)(1 + x)\right), \quad (9)$$

where $x = M_0 r$ and $K_1(x)$ is the McDonald function, has been used in [5]. For $T = T_c$ expressions (8) and (9) are almost indistinguishable. At $T > T_c$ the exact potential is slightly more attractive, the difference between (8) and (9) increases with T . Even more drastic approximation $V(r, T) \propto x K_1(x)$ was proposed [11]. This approximation was used in [5] to calculate the QQQ states.

3 Coulomb potential

We use the perturbative screened Coulomb potential (1) with the r -dependent QCD coupling constant $\alpha_s(r, T)$. Note that in the entire regime of distances, for which at $T = 0$ the heavy quark potential can be described well by QCD perturbation theory, $\alpha_s(r, T)$ remains unaffected by temperature effects at least up to $T \leq 3 T_c$ and agrees with the zero temperature running coupling $\alpha_s(r, 0) = \alpha_s(r)$. For our purposes, we find it convenient to define the r -dependent coupling constant in terms of the \mathbf{q}^2 -dependent constant $\alpha_B(\mathbf{q}^2)$ calculated in the background perturbation theory (BPT) [13]:

$$\alpha_s(r) = \frac{2}{\pi} \int_0^\infty dq \frac{\sin qr}{q} \alpha_B(\mathbf{q}^2). \quad (10)$$

The formula for $\alpha_B(\mathbf{q}^2)$ is obtained by solving the two-loop renormalization group equation for the running coupling constant in QCD

$$\alpha_B(\mathbf{q}^2) = \frac{4\pi}{\beta_0 t} \left(1 - \frac{\beta_1}{\beta_0^2} \frac{\ln t}{t}\right), \quad t = \ln \frac{\mathbf{q}^2 + m_B^2}{\Lambda_V^2}, \quad (11)$$

where β_i are the coefficients of the QCD β -function. The parameter $m_B \sim 1$ GeV has the meaning of the mass of the lowest hybrid excitation. The result can be viewed as arising from the interaction of a gluon with background vacuum fields. Note that $\alpha_B(r)$ increases with Λ_V and, for fixed Λ_V , decreases with m_B .

We employ the values $\Lambda_V = 0.36$ GeV, $m_B = 0.95$ GeV, which lie within the range determined in [14]. The result is consistent with the freezing of $\alpha_B(r)$ with a magnitude 0.563 (see Table 1 of [15]). The zero temperature potential with the above choice of the parameters gives a fairly good description of the quarkonium spectrum.

The Debye mass $m_D(T)$ in Eq. (1) is expressed in terms of the spatial string tension $\sigma_s(T)$ due to chromomagnetic confinement: $m_D(T) = 2.06\sqrt{\sigma_s(T)}$. The latter has been computed nonperturbatively up to two loops in the deconfined phase of QCD [7]. As was stated above, in this paper, we consider the pure-gauge $SU(3)$ theory ($T_c = 275$ MeV), for which m_D varies between 0.8 GeV and 1.4 GeV, when T varies between T_c and $2T_c$.

4 Results

4.1 Quark-antiquark states

In the framework of the FCM, the masses of heavy quarkonia are defined as

$$M_{Q\bar{Q}} = \frac{m_Q^2}{\mu_Q} + \mu_Q + E_0(m_Q, \mu_Q), \quad (12)$$

$E_0(m_Q, \mu_Q)$ is an eigenvalue of the Hamiltonian

$$H = H_0 + V_{np} + V_C, \quad (13)$$

m_Q are the bare quark masses, and einbeins μ_i are treated as c-number variational parameters. The eigenvalues $E_0(m_i, \mu_i)$ of the Hamiltonian (13) are found as functions of the bare quark masses m_i and einbeins μ_i , and are finally minimized with respect to the μ_i . With such simplifying assumptions the spinless Hamiltonian H_0 takes an apparently nonrelativistic form, with einbein fields playing the role of the constituent masses of the quarks. Once m_Q is fixed, the quarkonia spectrum is described. The dissociation points are defined as those temperature values for which the energy gap between $V(\infty, T)$ and $E_0(T)$ disappears.

In our calculations, we use the quark–antiquark potentials whose parameters are listed in Table 1. The potential I was employed in [5]. This potential uses the approximation (9) for $V(r)$ and the constant value $\alpha_s = 0.35$ for the Coulomb potential. The potential II is the same potential but with the running $\alpha_s(r)$ given by Eq. (10). In this case, we have slightly changed the parameter M_0 to preserve the value of $V(\infty, T_c) = 0.508$ GeV that agrees with lattice estimate for the free quark–antiquark energy¹. Note that for the potential in Eq. (9) the Bargmann integral (2) is

$$\frac{\mu_Q B}{M_0^4} \left(2 - 3\frac{T}{M_0}\right) \quad (14)$$

¹ However, the difference in the parameter M_0 causes the small difference of $V(\infty, T)$ for $T > T_c$, see tables 2, 3.

The potentials III and IV are defined by the exact integral representation (8) for $V(r)$ and correspond to the constant and running α_s , respectively.

We display in Figs. 1, 2 the binding energies of the 1S J/ψ and Υ mesons above the deconfinement temperature. The details of the calculation are presented in Tables 2, 3². In these tables we present the constituent quark masses μ_Q for $c\bar{c}$ and $b\bar{b}$, the binding energies $E_0 - V_{np}(\infty, T)$, the mean squared radii $r_0 = \sqrt{\langle r^2 \rangle}$, and the masses of the $Q\bar{Q}$ mesons. We employ $m_c = 1.4$ GeV and $m_b = 4.8$ GeV. As in the confinement region, the constituent masses μ_Q only slightly exceed the bare quark masses m_Q that reflect smallness of the kinetic energies of heavy quarks. We also mention that the account of the running $\alpha_s(r)$ in the Coulomb potential produces a tiny effect as compared with the case of a constant $\alpha_s = 0.35$ both for the energies (compare lines I and II and III and IV in Tables 2, 3) and $b\bar{b}$ wave functions in Fig. 3. Both for the charmonium and for the bottomonium states the energy gap $V(\infty, T) - E_0(T)$ gets smaller and the mean square radius r_0 gets larger as the temperature grows. We find no excited states 1P and 2S states, although the unbound 2S $b\bar{b}$ state appears to be very close to the threshold.

At $T = T_c$ we obtain the weakly bound $c\bar{c}$ state. The potential II predicts small additional binding ~ 20 MeV as compared with the binding for potential I. At $T = 1.3 T_c$ the difference of $V(\infty, T) - E_0(T)$ calculated for different potentials comprises only a few MeV. The melting temperature for the case IV is $\sim 1.3 T_c$. The charmonium masses lie in the interval 3.1–3.3 GeV, that agrees with the results of [12]. Note that immediately above T_c the mass of the $c\bar{c}$ state is about 0.2 GeV higher than that of J/ψ .

As expected, the Υ state is much more bound and remains intact up to the larger temperatures, $T \sim 2.3 T_c$ (all the details of calculation can be inferred from Table 3). The masses of the $L = 0$ bottomonium lie in the interval 9.7–9.8 GeV, about 0.2–0.3 GeV higher than 9.460 GeV, the mass of $\Upsilon(1S)$ at $T = 0$. At $T = T_c$ the $b\bar{b}$ separation r_0 is 0.25 fm, which is compatible with $r_0 = 0.28$ fm at $T = 0$. At the melting point $r_0 \rightarrow \infty$. Note that the 1S bottomonium undergoes very little modification till $T \sim 2 T_c$. The results agree with those found previously for a constant $\alpha_s = 0.35$ [5]. The melting temperatures for the J/ψ and Υ are shown in Table 4. The results for the Υ are in agreement with the lattice study of Ref. [16]. Note that in our calculations we neglect the spin-spin force, therefore the J/ψ and η_c mesons appear degenerate, as well as the Υ and η_b . This degeneracy is expected to be removed by a short range spin-spin interaction, whose effect, at $T = 0$, is often treated perturbatively assuming a contact interaction.

4.2 Dissociation of J/ψ and Υ in collision with gluons

Heavy quark bound states are important probes of the dynamics in the QGP. Charmonium suppression has been observed at a variety of energies at SPS [17] and RHIC [18]. While the melting of bound states certainly reduces quarkonium production, the converse is not true: different, even competing effects make it difficult to interpret charmonium suppression patterns. It has been noted that such effects should be less significant for bottomonium [19].

² In tables 2, 3 the results for the potential I that were previously reported in [5] are quoted for comparison.

Previous treatment of the dissociation of heavy quarkonium by the absorption of a gluon was carried out [20] using the operator product expansion in the the large N_c limit and hydrogen states to evaluate the transition matrix elements. In heavy quarkonia of interest, the radial dependence of the quark-antiquark potential and the corresponding wave functions differs from the Coulomb potential. The calculation of the dissociation cross section for a color $E1$ transition can be well described by the potential model, following the results of Akhiezer and Pomeranchuk [21] and Blatt and Weisskopf [22] obtained for the photo-disintegration of a deuteron. At low energies, the dominant dissociation cross section is the $E1$ color-electric dipole transition for which the quark final state will be the continuum $(Q\bar{Q})$ 1P state. We calculate the cross section for the quarkonium dissociation after a gluon impact similarly the calculation of the deuteron disintegration via the photon absorption as has been done in Refs. [23], [24].

An initial bound $(Q\bar{Q})_{1S}$ state with a binding energy $\varepsilon(T) = V(\infty, T) - E_0(T)$ relative to the threshold in the color-singlet potential ³ absorbs a $E1$ gluon of energy ω , and is excited to the color-octet final state $(Q\bar{Q})_{1P}$ with the energy

$$\frac{k^2}{\mu_Q} = \omega - \varepsilon(T). \quad (15)$$

The corresponding cross section reads

$$\sigma_{(Q\bar{Q})g}(\omega) = \frac{4\pi\alpha_{gQ}}{3} \frac{k^2 + k_0^2}{k} \left(\int_0^\infty u_{1P}(r) u_{1S}(r, T) r dr \right)^2, \quad (16)$$

where $u_{1S}(r, T)$ is the wave function of the $Q\bar{Q}$ bound state at the temperature T normalized as

$$\int_0^\infty |u_{1S}(r, T)|^2 dr = 1, \quad (17)$$

$\alpha_{gQ} = \alpha_s/6$, $u_{1P}(r)$ is the free P -wave $Q\bar{Q}$ wave function

$$u_{1P}(r) = \frac{\sin(kr)}{kr} - \cos(kr), \quad (18)$$

k is the momentum of outgoing quarks in Eq. (15), and

$$k_0^2 = 2\mu_Q \varepsilon(T). \quad (19)$$

The results are shown in Figs 4, 5. They are in a qualitative agreement with those of Ref. [23] where the $Q\bar{Q}$ potential was identified with the color singlet heavy quark free energy above T_c taken from quenched lattice QCD simulations.

4.3 QQQ baryons at $T \geq T_c$

The three-quark potential is given by

$$V_{QQQ} = \frac{1}{2} \sum_{i < j} V_{Q\bar{Q}}(r_{ij}, T), \quad (20)$$

³ $\varepsilon(T) \geq 0$ below the melting point.

where $\frac{1}{2}$ is the color factor. We solve the three-quark Schrödinger equation by the hyperspherical harmonics method. Using the three-body Jacobi coordinates

$$\boldsymbol{\rho} = \sqrt{\frac{\mu_Q}{2}} (\mathbf{r}_1 - \mathbf{r}_2), \quad \boldsymbol{\lambda} = \sqrt{\frac{2}{3}} \mu_Q \left(\frac{\mathbf{r}_1 + \mathbf{r}_2}{2} - \mathbf{r}_3 \right) \quad (21)$$

the wave function $\psi(\boldsymbol{\rho}, \boldsymbol{\lambda})$ in the hypercentral approximation is written as

$$\Psi(\boldsymbol{\rho}, \boldsymbol{\lambda}, T) = \frac{1}{\sqrt{\pi^3}} \frac{u(R, T)}{R^{5/2}}, \quad (22)$$

where the hyperradius

$$R^2 = \boldsymbol{\rho}^2 + \boldsymbol{\lambda}^2 = \frac{\mu_Q}{3} (r_{12}^2 + r_{23}^2 + r_{31}^2) \quad (23)$$

is invariant under quark permutations, and

$$\rho = R \sin \theta, \quad \lambda = R \cos \theta, \quad 0 \leq \theta \leq \pi/2. \quad (24)$$

Averaging the three-quark potential (20) over the six-dimensional sphere, one obtains the one-dimensional Schrödinger equation for the reduced function $u(R, T)$:

$$\frac{d^2 u(R, T)}{dR^2} + 2 \left[E_0 - \frac{15}{8 R^2} - \frac{3}{2} (\mathcal{V}_C(R, T) + \mathcal{V}(R, T)) \right] u(R, T) = 0, \quad (25)$$

where

$$\mathcal{V}_C(R, T) = -\frac{4}{3} \alpha_s \int_0^{\pi/2} \exp(-m_d(T) \hat{R}) \frac{d\Omega_6}{\hat{R}}, \quad (26)$$

$$\mathcal{V}(R, T) = V(\infty, T) - \frac{\xi(T)B}{M_0} \int_0^{\pi/2} \left(K_1(\hat{R}) \hat{R} - \frac{T}{M_0} e^{-\hat{R}} (1 + \hat{R}) \right) d\Omega_6, \quad (27)$$

$V(\infty, T)$ being given by Eq. (7), and

$$\hat{R} = \frac{M_0 R \sin \theta}{\mu_Q/2}, \quad d\Omega_6 = \frac{16}{\pi} \sin^2 \theta \cos^2 \theta d\theta. \quad (28)$$

The temperature-dependent mass of the colorless QQQ states is defined as

$$M_{QQQ} = \frac{3 m_Q^2}{2 \mu_Q} + \frac{3}{2} \mu_Q + E_0(m_Q, \mu_Q), \quad (29)$$

where μ_Q are now defined from the extremum condition imposed on M_{QQQ} in (29)

$$\frac{\partial M_{QQQ}}{\partial \mu_Q} = 0 \quad (30)$$

Note that the average interquark distances are

$$\sqrt{\langle r_{ij}^2 \rangle} = \sqrt{\frac{\langle R^2 \rangle}{\mu_Q}}, \quad (31)$$

see Eq. (23). The bound QQQ state exists if $E_0(m_Q, \mu_Q) \leq \mathcal{V}_{QQQ}(\infty, T)$, where

$$\mathcal{V}_{QQQ}(\infty, T) = \frac{3}{2} V(\infty, T). \quad (32)$$

In our three-quark calculations we use the potential I. For this potential there is no bound Ω_{ccc} states⁴. However, in all our calculations the Ω_{ccc} was found to lie almost at threshold. The Ω_{bbb} survives up to $T \sim 1.8 T_c$, see Table 5 and Fig. 6⁵.

5 Conclusions

In conclusion, we have calculated binding energies and melting temperatures for the lowest eigenstates in the $c\bar{c}$, $b\bar{b}$, and bbb systems. The color electric forces due to the nonconfining correlator D_1^E survive in the deconfined phase and they can support bound states at $T > T_c$. For what concerns the charm states, we find that J/ψ survive up to $T \sim 1.3 T_c$, and there is no bound Ω_c state at $T \geq T_c$. On the other hand, the $b\bar{b}$ and bbb states survives up to higher temperature, $T \sim 2.6 T_c$ and $T \sim 1.8 T_c$, respectively. This suggests that the systems are strongly interacting above T_c .

This work was supported in part by RFBR Grant 09-02-00629.

References

- [1] F. Karsch, M.T. Mehr and H. Satz, Z. Phys. C **37**, 617 (1988).
- [2] T. Matsui and H. Satz, Phys. Lett. B**178**, 416 (1986).
- [3] V. Bargmann, Proc. Nat. Acad. Sci. (USA), **38**, 961 (1952).
- [4] M. J. Tannenbaum, Rep. Prog. Phys. **69**, 2005 (2006).
- [5] I. M. Narodetskiy, Yu. A. Simonov, A. I. Veselov, JETP Lett. **90**, 232 (2009) [Pisma Zh. Eksp. Teor. Fiz. **90**, 254 (2009)].
- [6] A. V. Nefediev, Yu. A. Simonov, M. A. Trusov, Int. J. Mod. Phys. **E18**, 549 (2009).
- [7] N. O. Agasian, Phys. Lett. B**562**, 257 (2003) arXiv:0303127 [hep-ph].
- [8] I. M. Narodetskiy, Yu. A. Simonov, A. I. Veselov, AIP Conf. Proc. 1257: 804-807, 2009
- [9] I. M. Narodetskiy, Yu. A. Simonov, A. I. Veselov, arXiv:1012.0890 [hep-ph].

⁴The same should be true for the potential III, because at $T = T_c$ both potentials coincide. Moreover, since the effect of the running α_s and the change of the parameter M_0 is almost negligible, we conclude that Ω_{ccc} is unbound for all the potentials listed in Table 1.

⁵The small difference between the results reported in Table 5 and those of Table 4 of [5] is due to the difference of the r -dependent part of the nonperturbative quark-antiquark potential, see footnote 1.

- [10] Yu. A. Simonov, JETP Lett. **54**, 249 (1991), **55**, 605 (1992); Phys. Atom. Nucl. **58**, 309 (1995).
- [11] Yu. A. Simonov, Phys. Lett. B **619**, 293 (2005), Phys. Atom. Nucl. **69**, 528 (2006).
- [12] A. DiGiacomo, E. Meggiolaro, Yu. A. Simonov, and A. I. Veselov, Phys. Atom. Nucl. **70**, 908 (2007).
- [13] Yu. A. Simonov, Phys. Atom. Nucl. **58**, 107 (1995) [Yad. Fiz. **58**, 113 (1995)].
- [14] A. M. Badalian and D. S. Kuzmenko, Phys. Rev. D **65**, 016004 (2002).
- [15] R. Ya. Kezerashvili, I. M. Narodetskiy, and A. I. Veselov, Phys. Rev. D **79**, 034003 (2009).
- [16] G. Aarts et al., arXiv: 1010.3725 [hep-lat].
- [17] R. Arnaldi [NA60 Collaboration], Nucl. Phys. A **830**, 345C (2009).
- [18] A. Adare *et al.* [PHENIX Collaboration], Phys. Rev. Lett. **101**, 122301 (2008).
- [19] R. Rapp, D. Blaschke and P. Crochet, arXiv:0807.2470 [hep-ph].
- [20] M. E. Peskin, Nucl. Phys. B **156**, 365 (1979), G. Bhanot and M. E. Peskin, Nucl. Phys. B **156**, 391 (1979).
- [21] A. Akhieser and I. Pomeranchuk, *Some Problems of Atomic Nucleus Theory*, Moscow-Leningrad, 1948.
- [22] J. M. Blatt and V. F. Weisskopf, *Theoretical Nuclear Physics*, John Wiley and Sons, New York, 1952.
- [23] D. Blaschke, O. Kaczmarek, E. Laermann, V. Yudin, Eur. Phys. J. C **43**, 81 (2005).
- [24] Cheuk-Yin Wong, Phys. Rev. C **72**, 034906 (2005).

Table 1: Parameters of the non-perturbative quark-antiquark potentials described in the text. B and M_0 are in units GeV^3 and GeV , respectively. The potentials I-IV correspond to the value of $V(\infty, T_c) = 0.508 \text{ GeV}$

	$V(r)$	α_s^f	$\alpha_s(r)$	B	M_0
I	Eq. (9)	0.6	0.35	0.583	0.9
II	Eq. (9)	0.563	Eq.(10)	0.494	0.813
III	Eq. (8)	0.6	0.35	0.583	0.9
IV	Eq. (8)	0.563	Eq.(10)	0.494	0.813

Table 2: Details of the calculation of the $c\bar{c}$ states as a function of the temperature above the deconfinement region. $V(\infty, T)$, μ_c , $E_0 - V_{np}(\infty)$, and $M_{c\bar{c}}$ are given in units GeV , r_0 in units GeV^{-1} . $m_c = 1.4 \text{ GeV}$

T/T_c	Potential	$V(\infty, T)$	μ_c	$E_0 - V_{np}(\infty)$	r_0	$M_{c\bar{c}}$
1	I	0.508	1.451	- 0.019	7.53	3.291
	II	0.509	1.469	- 0.040	6.07	3.271
	III	0.508	1.454	- 0.022	7.24	3.288
	IV	0.509	1.473	- 0.048	5.75	3.264
1.3	I	0.381	1.419	+ 0.006	10.50	3.186
	II	0.372	1.425	+ 0.001	9.75	3.173
	III	0.381	1.424	+ 0.001	9.91	3.183
	IV	0.372	1.434	- 0.008	8.72	3.165
1.6	IV	0.262	1.416	+ 0.007	10.74	3.069

Table 3: Details of the calculation of the $b\bar{b}$ states as a function of the temperature above the deconfinement region. The notations are the same as in Table 2, $m_b = 4.8$ GeV

T/T_c	Potential	$V(\infty, T)$	μ_b	$E_0 - V_{np}(\infty)$	r_0	$M_{b\bar{b}}$
1	I	0.508	4.984	- 0.300	1.27	9.815
	II	0.508	4.953	- 0.315	1.32	9.798
	III	0.508	4.985	- 0.308	1.26	9.807
	IV	0.509	4.953	- 0.326	1.31	9.786
1.3	I	0.381	4.950	- 0.183	1.55	9.802
	II	0.372	4.925	- 0.187	1.61	9.788
	III	0.381	4.953	- 0.200	1.51	9.785
	IV	0.372	4.928	- 0.211	1.55	9.764
1.6	I	0.275	4.915	- 0.095	2.06	9.783
	II	0.262	4.896	- 0.093	2.14	9.772
	III	0.275	4.921	- 0.119	1.91	9.759
	IV	0.262	4.902	- 0.126	1.94	9.739
2.0	I	0.162	4.863	- 0.021	4.25	9.742
	II	0.146	4.851	- 0.017	4.66	9.729
	III	0.162	4.878	- 0.046	3.03	9.717
	IV	0.146	4.866	- 0.048	3.05	9.698
2.2	I	0.115	4.832	- 0.003	7.62	9.712
	II	0.097	4.823	- 0.001	8.51	9.696
	III	0.115	4.855	- 0.023	4.32	9.693
	IV	0.097	4.847	- 0.023	4.34	9.674
2.3	I	0.093	4.818	+ 0.001	9.52	9.694
	II	0.075	4.813	+ 0.002	10.17	9.677
2.4	III	0.073	4.831	- 0.007	6.80	9.665
	IV	0.054	4.827	- 0.007	6.91	9.648
2.6	III	0.034	4.812	+ 0.001	9.91	9.635
	IV	0.016	4.809	+ 0.001	10.18	9.617

Table 4: Dissociation temperatures (in units of T_c) for $c\bar{c}$ and $b\bar{b}$ states

	I	II	III	IV
J/ψ	1.24	1.29	1.29	1.46
Υ	2.27	2.29	2.57	2.57

Table 5: Details of the calculation of bbb baryon above the deconfinement region for the potential I of Table 1. $\mathcal{V}_{QQQ}(\infty, T)$ is defined by Eq. (32). $\sqrt{R^2}$ is related to the interquark distances by Eq. (31). Dimensions are the same as in Table 2. $m_b = 4.8$ GeV

$\frac{T}{T_c}$	$\mathcal{V}_{QQQ}(\infty, T)$	μ_b	$E_0 - \mathcal{V}(\infty, T)$	$\sqrt{R^2}$	M_{bbb}
1	0.763	4.943	- 0.279	3.73	14.890
1.3	0.571	4.906	- 0.135	4.80	14.840
1.6	0.414	4.865	- 0.037	7.17	14.777
1.8	0.324	4.835	+ 0.001	10.00	14.724

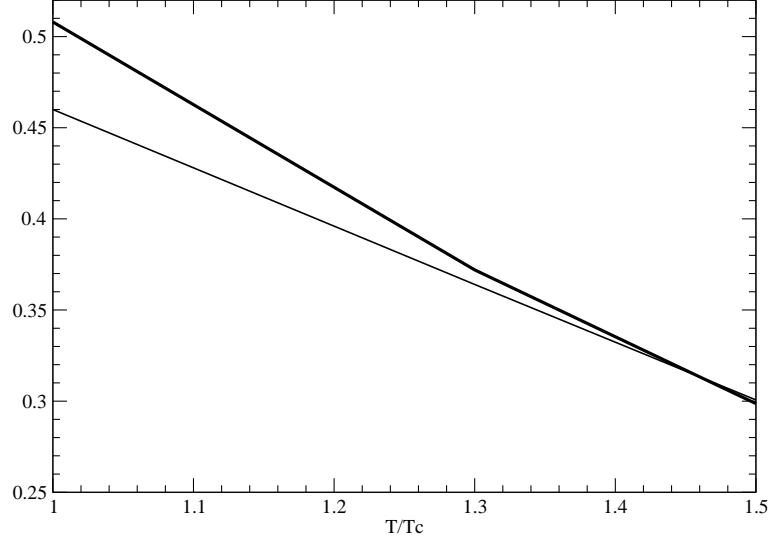


Figure 1: $V(\infty, T)$ (thick curve) and $E_0(T)$ (thin curve) are plotted against T/T_c for the J/ψ (the potential IV). $V(\infty, T)$ and $E_0(T)$ are given in units of GeV.

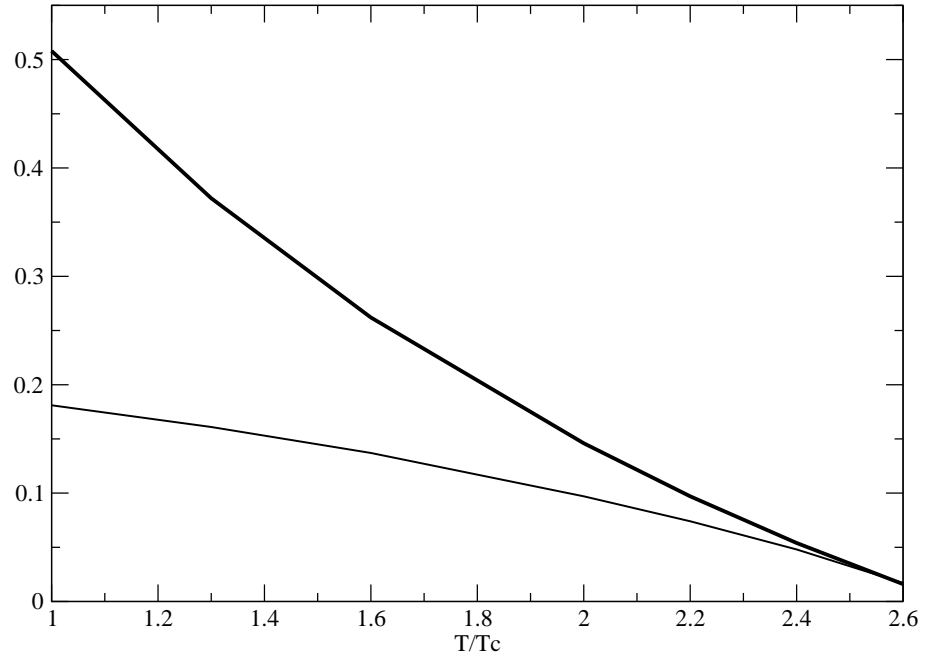


Figure 2: The same as in Fig. 1 for the ground Υ state

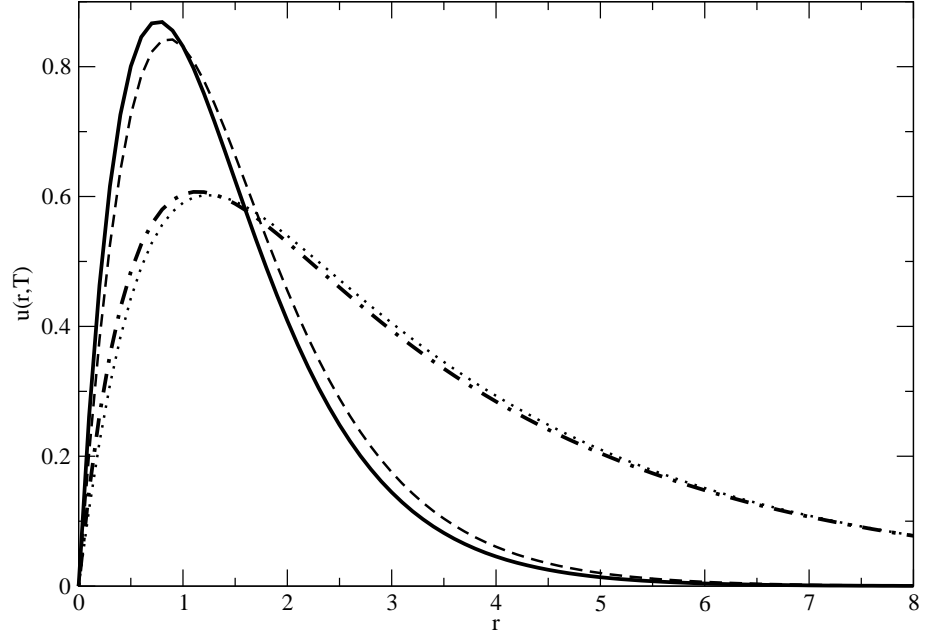


Figure 3: The $\bar{b}b$ wave function $u(r, T)$ normalized to unity (r in units of GeV^{-1}). Solid and dashed curves show the $u(r, T_c)$ for the potential I and II, respectively, dot-dashed and dot curves show the $u(r, 2T_c)$ for the potentials I and II.

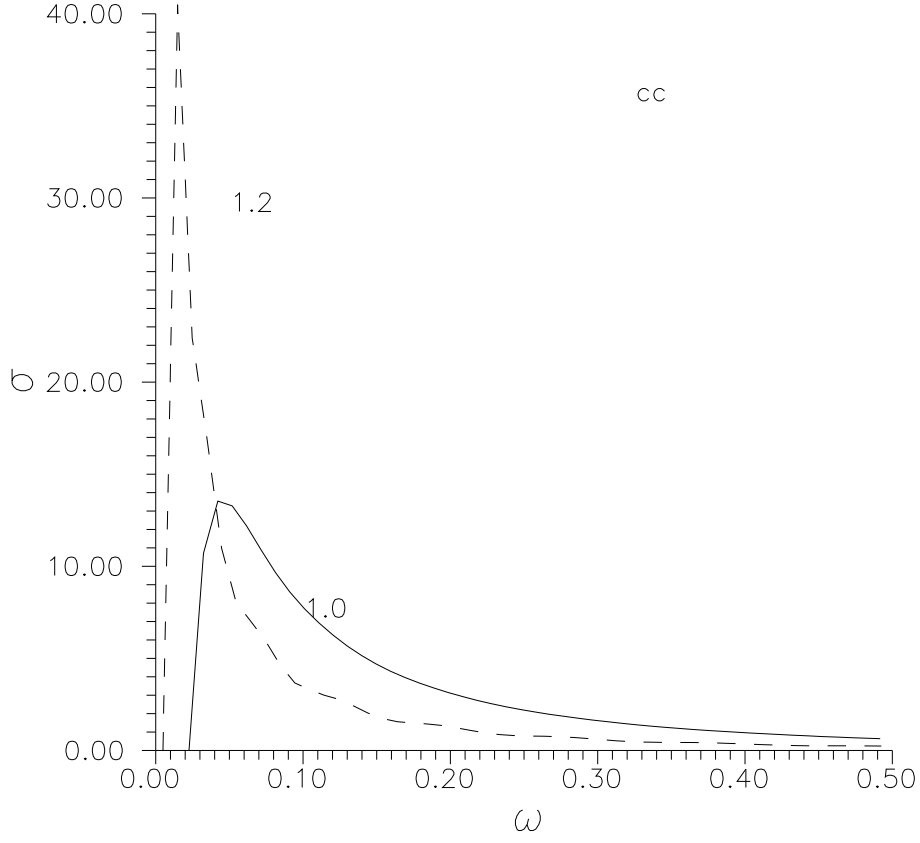


Figure 4: Cross sections σ for J/ψ dissociation in the potential model vs gluon energy ω . The curves are labelled by the ratios T/T_c . σ and ω are given in units GeV^{-2} and GeV , respectively.

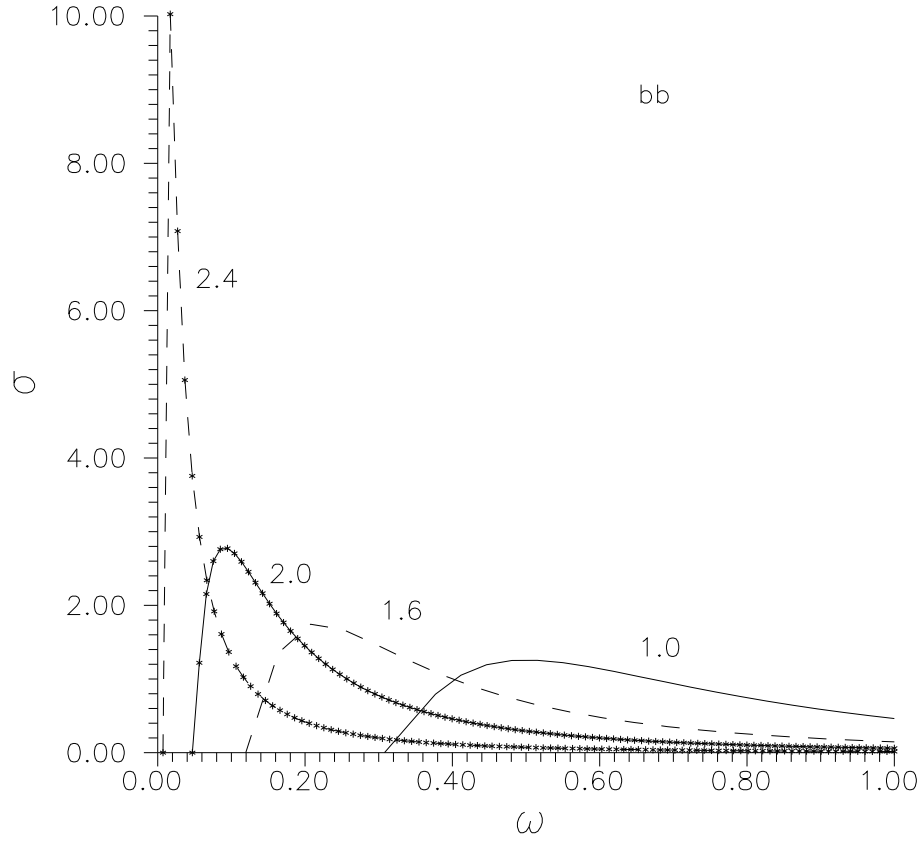


Figure 5: Cross sections for $b\bar{b}$ dissociation in the potential model. The notations are the same as in Fig. 4

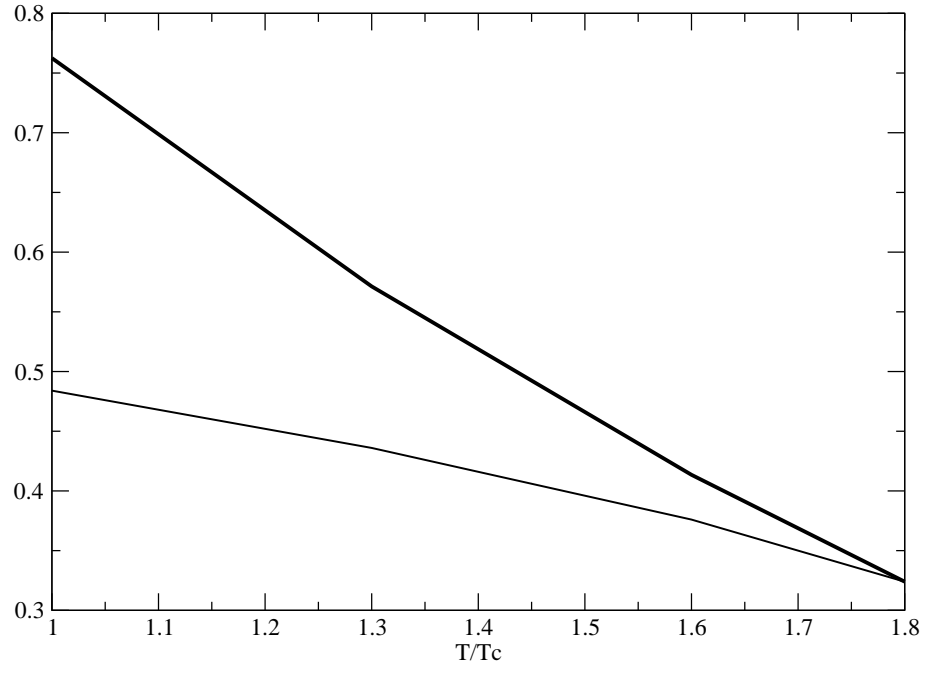


Figure 6: $\mathcal{V}(\infty, T)$ (thick curve) and $E_0(T)$ (thin curve) in units of GeV for the Ω_{bbb} (the potential I)